Cell

RYBP-PRC1 Complexes Mediate H2A Ubiquitylation at Polycomb Target Sites Independently of PRC2 and H3K27me3

Lígia Tavares,[1] Emilia Dimitrova,[2] David Oxley,[3] Judith Webster,[3] Raymond Poot,[4] Jeroen Demmers,[5] Karel Bezstarosti,[5] Stephen Taylor,[6] Hiroki Ura,[7] Hiroshi Koide,[7] Anton Wutz,[8] Miguel Vidal,[9] Sarah Elderkin,[2,*] and Neil Brockdorff[1,*]
[1]Department of Biochemistry, University of Oxford, South Parks Road, Oxford OX1 3QU, UK
[2]Nuclear Dynamics
[3]Mass Spectrometry
Babraham Institute, Babraham Research Campus, Cambridge CB22 3AT, UK
[4]Department of Cell Biology
[5]Proteomics Center
Erasmus Medical Center, Dr. Molewaterplein 50, 3015GE Rotterdam, The Netherlands
[6]Computational Biology Research Group, WIMM, University of Oxford, John Radcliffe Hospital, Headington, Oxford OX3 9DS, UK
[7]Department of Stem Cell Biology, Graduate School of Medical Science, Kanazawa University, 13-1 Takaramachi, Kanazawa, Ishikawa 920-8640, Japan
[8]Wellcome Trust Centre for Stem Cell Research, Tennis Court Road, Cambridge CB2 1QR, UK
[9]Cell Proliferation and Development, Centro de Investigaciones Biológicas, Consejo Superior de Investigaciones Cientificas (CSIC), 28040 Madrid, Spain
*Correspondence: sarah.elderkin@babraham.ac.uk (S.E.), neil.brockdorff@bioch.ox.ac.uk (N.B.)
DOI 10.1016/j.cell.2011.12.029

SUMMARY

Polycomb-repressive complex 1 (PRC1) has a central role in the regulation of heritable gene silencing during differentiation and development. PRC1 recruitment is generally attributed to interaction of the chromodomain of the core protein Polycomb with trimethyl histone H3K27 (H3K27me3), catalyzed by a second complex, PRC2. Unexpectedly we find that RING1B, the catalytic subunit of PRC1, and associated monoubiquitylation of histone H2A are targeted to closely overlapping sites in wild-type and PRC2-deficient mouse embryonic stem cells (mESCs), demonstrating an H3K27me3-independent pathway for recruitment of PRC1 activity. We show that this pathway is mediated by RYBP-PRC1, a complex comprising catalytic subunits of PRC1 and the protein RYBP. RYBP-PRC1 is recruited to target loci in mESCs and is also involved in Xist RNA-mediated silencing, the latter suggesting a wider role in Polycomb silencing. We discuss the implications of these findings for understanding recruitment and function of Polycomb repressors.

INTRODUCTION

Polycomb-group (PcG) repressor proteins play a key role in establishing and maintaining gene expression patterns during cellular differentiation and development. There are two major biochemical complexes, PRC1 and PRC2, that have inherent histone-modifying activity critical for their function in gene repression, monoubiquitylation of histone H2AK119 (H2AK119u1), and di- tri-methylation of histone H3K27, respectively (reviewed in Müller and Verrijzer, 2009). Mechanisms other than H2A ubiquitylation also contribute to PRC1-mediated gene repression (Eskeland et al., 2010; Francis et al., 2001, 2004; King et al., 2002; Shao et al., 1999). In mammals the catalytic RING1A/B subunit of PRC1 is also found in the E2F6 (Ogawa et al., 2002; Sánchez et al., 2007; Trimarchi et al., 2001) and BCOR (Gearhart et al., 2006; Sánchez et al., 2007) complexes. An atypical PRC1 complex, dRAF, comprising the proteins dRING, PSC, and the histone demethylase KDM2 has been identified in *Drosophila* (Lagarou et al., 2008).

Genetic analyses have demonstrated that PcG target loci are often coregulated by PRC1 and PRC2, and consistent with this, genome mapping studies in *Drosophila* and mouse demonstrate co-occupancy of PRC1 and PRC2 at many PcG target loci (Boyer et al., 2006; Ku et al., 2008; Schwartz et al., 2006). Co-occupancy is thought to be a consequence of recruitment of PRC1 via interaction of the chromodomain in the PRC1 protein PC (mammalian homologs CBX2/4/6/7/8) with PRC2-dependent H3K27me3. This is based on biochemical studies demonstrating binding of the PC chromodomain to H3K27me3 (Cao et al., 2002; Fischle et al., 2003; Min et al., 2003) and on genetic analyses demonstrating displacement of PRC1 proteins from chromatin in PRC2 mutants (Boyer et al., 2006; Cao et al., 2002; Wang et al., 2004). The idea has been further substantiated in studies demonstrating a direct link between H3K27me3 and PRC1 recruitment (Agger et al., 2007; Lee et al., 2007; Mujtaba et al., 2008).

Although the hierarchical model for PRC1 recruitment is widely accepted, there are specific examples where PRC1/H2AK119u1 targeting is independent of H3K27me3 (reviewed

in Simon and Kingston, 2009). Notably, in PRC2-depleted mouse embryonic stem cells (mESCs) (Leeb et al., 2010), and differentiated cells (Pasini et al., 2007), PRC1 proteins have been detected at selected target loci, and moreover, global H2AK119u1 levels are similar to those of wild-type (WT) cells (Schoeftner et al., 2006). Related observations also conflict with hierarchical recruitment. In mESCs, targeting of PRC2 and PRC1 to promoters of key regulators of embryonic lineages is thought to restrain differentiation (Azuara et al., 2006; Boyer et al., 2006; Mikkelsen et al., 2007; Stock et al., 2007). Arguing against this, PRC2-deficient mESCs remain undifferentiated and show only minimal upregulation of PcG target loci (Boyer et al., 2006; Chamberlain et al., 2008; Leeb et al., 2010; Shen et al., 2008). Conversely, PRC1-deficient mESCs strongly upregulate PcG target loci and differentiate spontaneously (Endoh et al., 2008; Stock et al., 2007).

In this study, we investigated PRC1 recruitment in PRC2 null mESCs. We show that in the absence of H3K27me3, PRC1 catalytic subunits occupy the majority of PcG target loci, albeit at reduced levels. This recruitment confers near normal levels of H2AK119u1. We further demonstrate that H3K27me3-independent H2AK119u1 is mediated by a PRC1-related complex, RYBP-PRC1, comprising PRC1 catalytic subunits and the protein RYBP.

RESULTS

H2AK119u1 and PRC1 Subunits Localize to PcG Target Genes in *Eed*$^{-/-}$ ESCs

To investigate the importance of H3K27me3 in PRC1 recruitment in mESCs, we performed ChIP for selected PcG target loci in *Eed*$^{-/-}$ mESCs that lack H3K27me3. In addition to loci repressed by PcG proteins, we analyzed loci that are expressed in mESCs, loci that are widely expressed, and a locus that is repressed in mESCs independently of PcG activity. As shown in Figure 1A, H3K27me3 was depleted in *Eed*$^{-/-}$ mESCs, and there was a greatly reduced occupancy of the PRC1 core proteins RING1B and MEL-18 compared to *Eed*$^{+/+}$ mESCs. These observations are broadly consistent with hierarchical recruitment of PRC1 by H3K27me3. However, low levels of RING1B/MEL-18 were detectable at PcG target loci in *Eed*$^{-/-}$ cells, and moreover, significant levels of H2AK119u1 were also present (Figure 1A, lower panel). Additionally, global levels of H2AK119u1 were apparently unaffected (Figure 1B).

Similar results were obtained using a conditional knockout (cKO) *Eed*$^{-/-}$ ESC line, Eed4, in which *Eed* is repressed when doxycycline is added to the culture medium (Ura et al., 2008). Treatment of Eed4 cells with doxycycline for 15 days did not affect mESC pluripotency (Figures S1A and S1B available online). Western blot analysis demonstrated that EED protein and H3K27me3 were fully depleted (Figure S1C). Levels of PRC2 core proteins EZH2 and SUZ12 were also strongly reduced (Figure S1C), consistent with previous observations (Pasini et al., 2007). In contrast, global levels of H2AK119u1 were broadly unchanged, as were levels of RING1B (Figure S1C). Analysis of defined PcG target genes by ChIP demonstrated depletion of H3K27me3 and retention of H2AK119u1, albeit at moderately reduced levels (Figure S1D). That lower levels of H2AK119u1 occur at target loci relative to constitutive *Eed*$^{-/-}$ cells (Figure 1A) may indicate that enhanced H2AK119u1 is favored by cell selection during derivation and long-term culture. These results confirm that maintenance of H2AK119u1 in mESCs occurs independently of PRC2 and associated H3K27me3.

RING1B Is Retained at the Majority of PcG Targets in the Absence of H3K27me3

Conventional ChIP analysis indicated that low levels of the core PRC1 proteins RING1B and MEL-18 are present at selected PcG targets following depletion of H3K27me3 in mESCs (Figure 1A). To extend this we carried out RING1B ChIP-sequencing (ChIP-seq) in *Eed*$^{+/+}$ and *Eed*$^{-/-}$ ESCs. H3K27me3 ChIP-seq was carried out as a control. *Irx2, Msx1* (Figure 2A), and *HoxD* (Figure S2A) are examples of defined PcG targets in mESCs (Mikkelsen et al., 2007). RING1B binding is readily detectable in *Eed*$^{+/+}$ cells and also in *Eed*$^{-/-}$ cells, albeit at much lower levels. To compensate for the reduced signal, we increased the number of reads for the *Eed*$^{-/-}$ RING1B and input samples by approximately 4-fold (Figures 2A and S2A, x4 tracks). This revealed that the broad pattern of RING1B occupancy, mapping to target loci-associated CpG islands, is retained in *Eed*$^{-/-}$ mESCs. Non-PcG target loci, for example *Oct3/4*, a gene that is expressed in ESCs, and *Gata1*, a gene that is silenced independently of PcG, do not show RING1B occupancy either in *Eed*$^{+/+}$ or *Eed*$^{-/-}$ ESCs (Figure 2A).

Using model-based analysis of ChIP-Seq (MACS) to identify peaks, we found 2,347 places where RING1B is enriched in *Eed*$^{+/+}$ cells, and in comparison 1,810 places in *Eed*$^{-/-}$ cells. Fifty-three percent of regions bound by RING1B in the *Eed*$^{+/+}$ ESCs are also targets in the mutant cells (Figure 2B). We consider this to be an underestimate as the thresholds used fail to detect some RING1B peaks over background in *Eed*$^{-/-}$ cells. For example, at the 3′ end of the *Wnt6* locus, MACS records a RING1B peak only for *Eed*$^{+/+}$ ESCs, but a similar peak pattern centered on associated CpG islands is seen also in *Eed*$^{-/-}$ ESCs (Figure S2B, left panel). In other cases, for example the *Tbkbp1* locus (Figure S2B, right panel), RING1B peaks recorded in *Eed*$^{+/+}$ ESCs are broad and detected only at a low level. In *Eed*$^{-/-}$, this pattern can be observed when comparing to input sample but is not recognized as a peak due to increased background relative to signal. Examples of peaks detected in *Eed*$^{-/-}$ but not *Eed*$^{+/+}$ cells are shown in Figure S2C. In some cases, for example *Sfmbt1*, RING1B occupancy is similar in *Eed*$^{+/+}$ and *Eed*$^{-/-}$ samples, whereas in others, for example *Socs3*, only very low levels of RING1B occupancy are apparent in the *Eed*$^{+/+}$ samples. It is probable that in these examples H3K27me3 is less important for RING1B binding.

The distribution of peaks across transcription start sites (TSS) is similar in *Eed*$^{+/+}$ and *Eed*$^{-/-}$, in both cases being within ± 1 Kb from the TSS (Figure 2C). Gene ontology (GO) analysis demonstrates no significant differences between target loci in *Eed*$^{+/+}$ and *Eed*$^{-/-}$ samples (Figure 2D).

As noted previously for *Eed*$^{+/+}$ cells (Ku et al., 2008) and above (Figures 2 and S2), many of the PcG target regions are CpG islands, with 99% of peaks shared between *Eed*$^{+/+}$ and *Eed*$^{-/-}$ cells overlapping with CpG islands (Figure 2E). The few exceptions that we found (13 peaks) are regions with high GC content

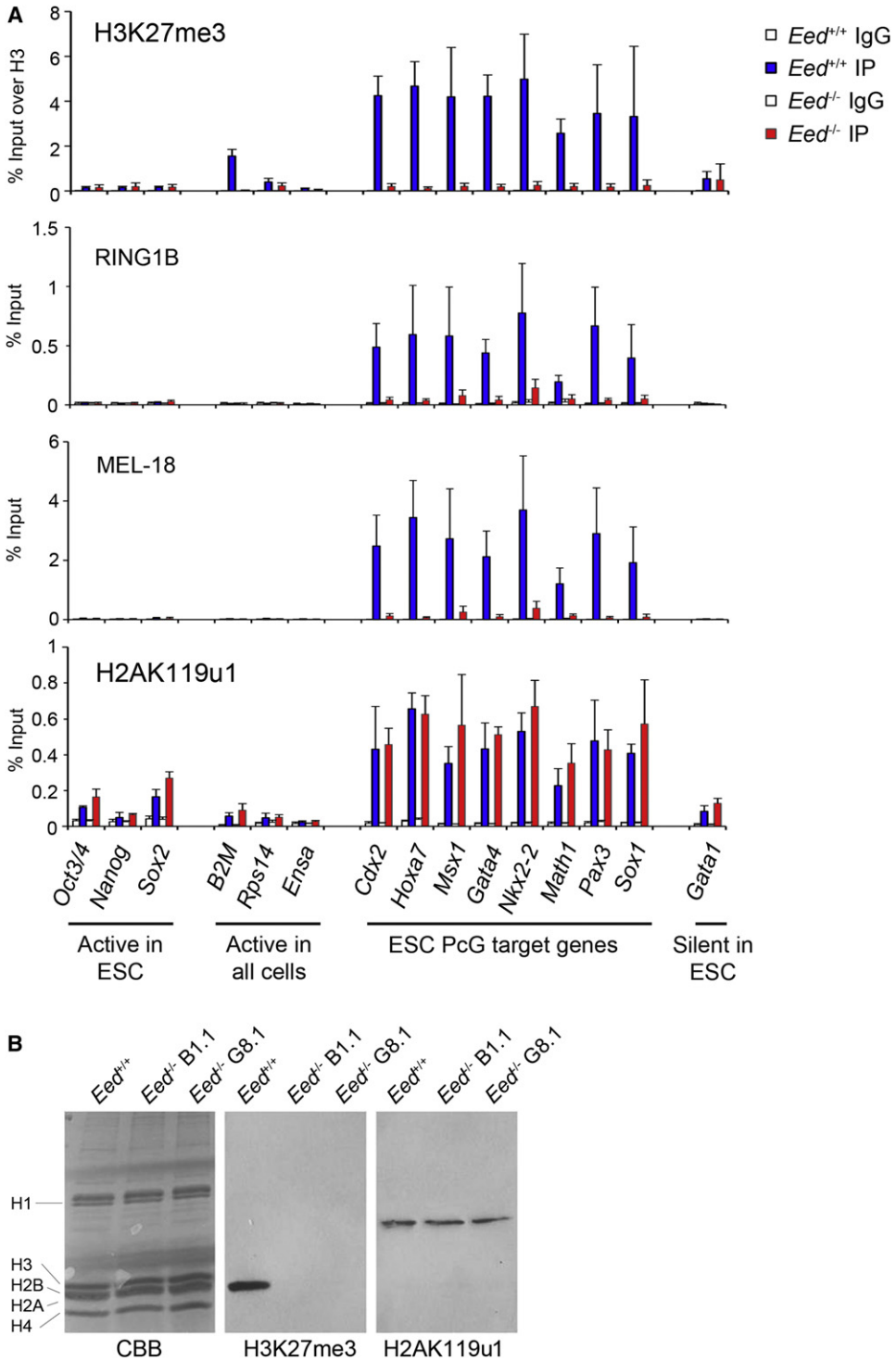

Figure 1. Retention of H2AK119u1 at PcG Target Loci in *Eed*$^{-/-}$ mESCs

(A) ChIP analysis of H3K27me3, RING1B, MEL-18, and H2AK119u1 in wild-type (*Eed*$^{+/+}$) and *Eed*$^{-/-}$ mESCs. Bars show average + SD, n = 3.

(B) Western blot analysis of histone extracts showing absence of H3K27me3 and retention of H2AK119u1 in two independent *Eed*$^{-/-}$ mESC cell lines, B1.1 and G8.1. CBB (Coomassie brilliant blue).

See also Figure S1.

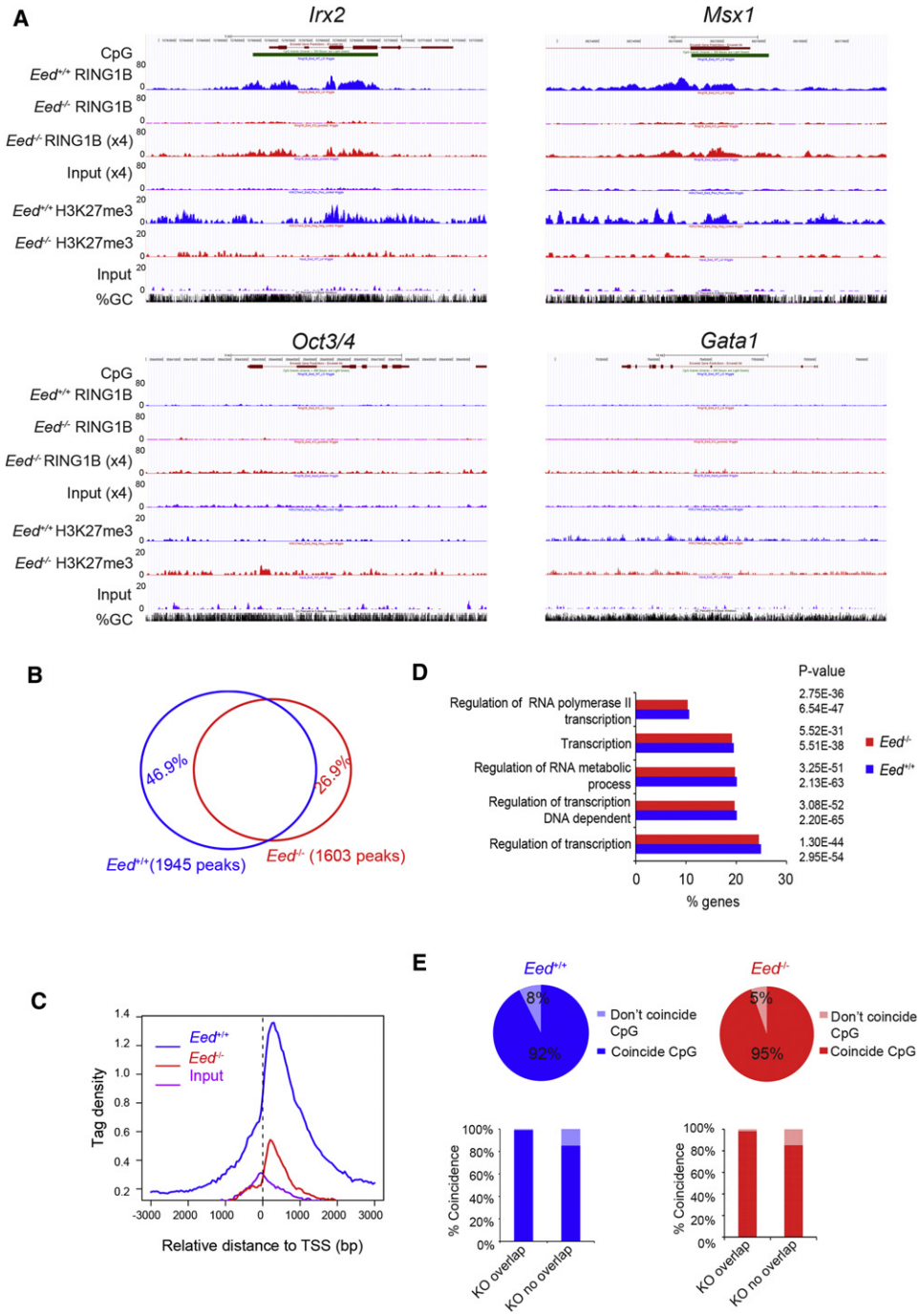

Figure 2. ChIP-Seq Demonstrates RING1B Occupancy at PcG Target Loci in *Eed*$^{+/+}$ and *Eed*$^{-/-}$ mESCs

(A) Example screen shots for *Eed*$^{+/+}$ IP (blue) and *Eed*$^{-/-}$ IP (red) and input (lilac). *Irx2* and *Msx1* are PcG targets. *Oct3/4* and *Gata1* are non-PcG targets.

(B) Venn diagram indicating overlap of RING1B peaks (genes) in *Eed*$^{+/+}$and *Eed*$^{-/-}$ cells.

(C) Tag density in relation to TSS of 20 million reads randomly subsampled.

(D) Comparison showing similarity in gene ontology distribution for peaks in *Eed*$^{+/+}$ and *Eed*$^{-/-}$ mESCs.

(E) Co-incidence of peaks with CpG islands for *Eed*$^{+/+}$ and *Eed*$^{-/-}$ mESCs (above) and the proportion of peaks coinciding with CpG islands in overlapping and nonoverlapping subgroups defined in (B).

See also Figure S2.

that are not annotated as CpG islands. Interestingly, a high proportion of the nonoverlapping peaks also coincide with CpG islands (Figures 2E and S2C). Co-occurrence of RING1B sites and CpG was shown to be significant ($p < 0.001$, co-occurrence of R test; Huen and Russell, 2010). Taken together these results demonstrate extensive overlap of RINGB targets in mESCs lacking H3K27me3 relative to WT cells.

Re-recruitment of PRC1 Activity to PcG Target Loci following Depletion of H2AK119u1

PRC2 occupancy and H3K27me3 can be maintained at an ectopic site following withdrawal of the primary recruitment signal (Hansen et al., 2008), possibly via binding of an aromatic cage in EED to H3K27me3 (Margueron et al., 2009). With this in mind, we considered that although primary recruitment of PRC1 may require PRC2-mediated H3K27me3, H2AK119u1, once established, could function as a signal for maintenance of PRC1 occupancy. To address this, we used the reversible proteasome inhibitor MG132 (Dantuma et al., 2006) to deplete H2AK119u1 in Eed4 cells in the presence or absence of PRC2 and then determined whether restoration of H2AK119u1 occurs following withdrawal of the inhibitor. Secondary effects of MG132 treatment on mESCs are negligible with the described conditions (Szutorisz et al., 2006). As shown in Figure 3A, treatment of cells with MG132 for 6 hr efficiently depleted global H2AK119u1 (lanes 2 and 6). Allowing cells to recover for 3 days after withdrawal of the inhibitor resulted in restoration of H2AK119u1 in both the presence and the absence of H3K27me3 (lanes 4 and 8, respectively), and this was also the case after only 1 day of recovery (Figure S3A). ChIP analysis demonstrated that H2AK119u1 accumulates appropriately at PcG target loci after recovery, with levels being slightly reduced in the absence of H3K27me3 (Figure 3B). Recruitment of RING1B and EZH2 was retained following MG132 treatment, albeit at a slightly reduced level (Figure S3B).

Expression analysis (Figure 3C) demonstrated that treatment with MG132 derepresses PcG target loci in both the presence and the absence of H3K27me3, and that silencing is restored following withdrawal of the inhibitor. No effect was seen at the *Gata1* locus at which repression is PcG independent. Initiation of differentiation due to H2AK119u1 depletion (Endoh et al., 2008; Stock et al., 2007) accounts for the reduced levels of expression of pluripotency factors following MG132 treatment. Derepression of PcG targets was enhanced in the absence of H3K27me3, consistent with lower H2AK119u1 when MG132 treatment was begun (see Figure S1C). Taken together these results demonstrate that de novo deposition of H2AK119u1 in mESCs occurs appropriately at known PcG target loci in both the presence and the absence of H3K27me3.

RYBP Is a Stoichiometric Component of PRC1 in ESCs

To explore the mechanism of H3K27me3-independent targeting of H2AK119u1, we carried out a proteomic screen for PRC1-associated proteins in mESCs. Because RING1B associates with non-PRC1 complexes (Gearhart et al., 2006; Ogawa et al., 2002; Sánchez et al., 2007; Trimarchi et al., 2001), we analyzed the core PRC1 protein MEL-18, a close homolog of the *Drosophila* PRC1 protein PSC that is highly expressed in mESCs (Elderkin et al., 2007) and moreover localizes to PcG target loci, albeit at low levels, in H3K27me3-deficient mESCs (Figure 1A). We established ESC lines expressing epitope-tagged MEL-18 and purified associated proteins. In liquid chromatography-tandem mass spectrometry (LC-MS/MS) experiments, we identified core PRC1 proteins, specifically RING1A/RING1B, MPH1/2/3, CBX2/7/8, and in addition, RYBP, a factor previously shown to interact with RING1A/B (Czypionka et al., 2007; Endoh et al., 2008; García et al., 1999; Wang et al., 2010) and also with the transcription factor YY1 (García et al., 1999) (Figure S4A). Identification of specific bands on silver-stained gels indicated stoichiometric amounts of PRC1 proteins and RYBP (Figures 4A, panels 1 and 2 and 4B). These findings were further substantiated by western analysis (Figure 4C, panels 1 and 2). Notably, LC-MS/MS did not detect YY1 (Figure 4B). This was confirmed by western analysis (Figure 4C and see below).

To determine whether association of MEL-18 with RYBP occurs in cells other than mESCs, we expressed MEL-18-FLAG in neural stem cells (NSCs) and again purified associated proteins (Figure S4B). LC-MS/MS/western analysis identified the major PRC1 proteins RING1A/B, CBX2/4/7/8, and MPH1 and, additionally, high levels of RYBP. Thus, association of RYBP with MEL-18 complexes is not cell type specific.

We used size-exclusion chromatography to further analyze mESC MEL-18-associated complexes (Figure S4C). Peaks for MEL-18, RING1B, RYBP, and CBX7 were centered over fractions corresponding to 150–200 kDa. A similar elution profile was observed for RING1B, RYBP, and CBX7 following size-exclusion chromatography of nuclear extracts, both from *Eed*$^{+/+}$ and *Eed* $^{-/-}$ mESCs (Figure S4D). These observations point to involvement of RYBP in a multiprotein complex(es) with core PRC1 proteins.

Distinct PRC1 Complexes Defined by Mutually Exclusive Binding of RYBP or CBX7 to RING1B

Although RYBP has been identified as a component of E2F6 (Ogawa et al., 2002; Sánchez et al., 2007; Trimarchi et al., 2001) and BCOR (Gearhart et al., 2006; Sánchez et al., 2007), complexes that both also include RING1A/B proteins, it was not previously recognized as a component of conventional PRC1 complexes. Indeed this result is unexpected in light of structural studies that demonstrate that both RYBP and CBX proteins interact with the same surface on the RING1B protein, and that their binding is therefore mutually exclusive (García et al., 1999; Wang et al., 2010). To examine this further, and to confirm these interactions in native complexes from WT and *Eed*-deficient (Eed4 cKO) mESCs, we carried out coimmunoprecipitation (coIP) experiments with antisera to RING1B, MEL-18, RYBP, and CBX7 (Figures 5A and S5A). Immunoprecipitates were treated with either benzonase or ethidium bromide (EtBr) to confirm that interactions are not mediated by nucleic acid binding. Both RING1B and MEL-18 coIP core PRC1 proteins, i.e., RING1B, MEL-18, MPH1, CBX7, and additionally RYBP, consistent with analysis of MEL-18-Flag affinity purifications (Figure 5A, panels 1 and 2). RING1B, MEL-18, low levels of MPH1, but not CBX7 coIP with RYBP (Figure 5A, panel 3). Conversely, RING1B, MEL-18, and MPH1 but not RYBP coIP with CBX7 (Figure 5A, panel 4). No differences were observed

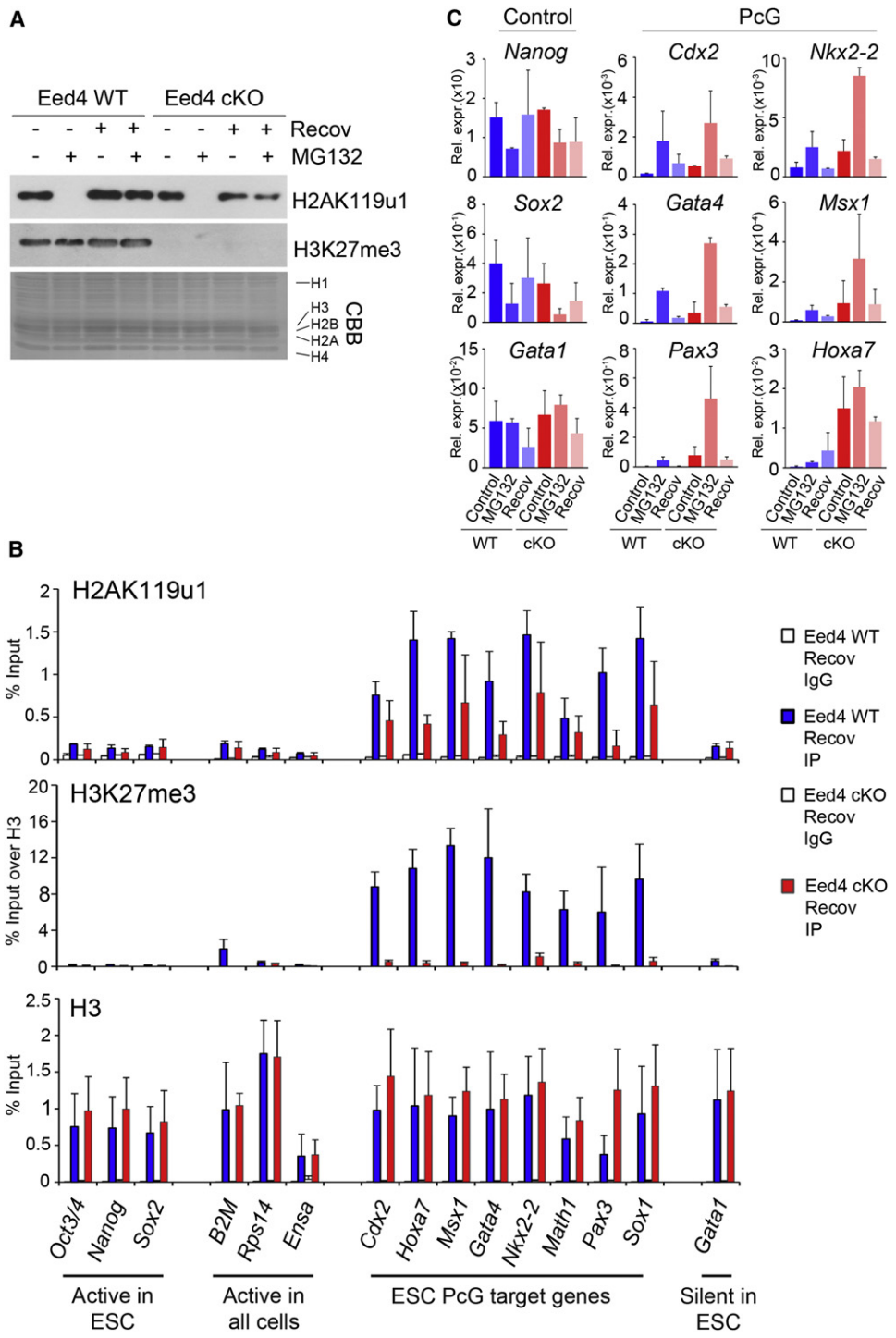

Figure 3. H2AK119u1 Is Re-established following Depletion in Eed4 WT and Eed4 cKO mESCs

(A) Western blot for H2AK119u1 and H3K27me3 in histone extracts. CBB: Coomassie brilliant blue. H2AK119u1 is completely depleted after 6 hr with 10 μM MG132 and is then restored when cells are left to recover (recov) for 3 days after inhibitor removal, irrespective of presence of H3K27me3.

(B) ChIP for H2AK119u1 and H3K27me3 in Eed4 WT and Eed4 cKO cells. H3 is shown as a control. Bars show average + SD, n = 3.

(C) Expression analysis (Rel. expr.) of selected loci. For RT-PCR analysis, values were normalized against the average of three housekeeping genes, *Hmbs*, *Gapdh*, and *Idh1*. Bars show average + SD, n = 3.

See also Figure S3.

A

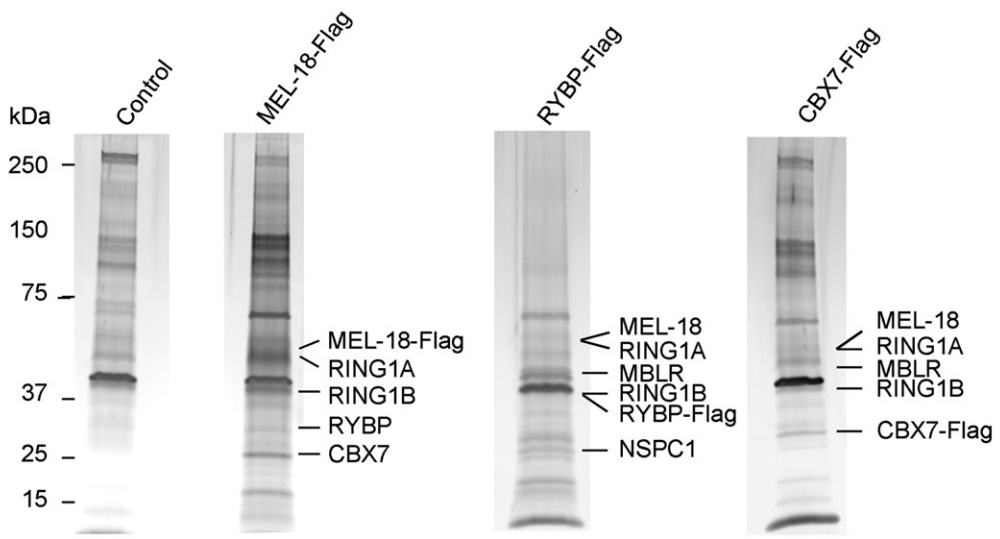

B

		MEL-18-Flag			RYBP-Flag			CBX7-Flag		
Protein	Accession	Mascot [1]	% Cover	Peptides [2]	Mascot [1]	% Cover	Peptides [2]	Mascot [1]	% Cover	Peptides [2]
RING1B	gi/33563274	911	72	20	509	42	10	932	44	12
MEL-18	gi/6678635	785	51	22	267	33	8	440	50	18
RING1A	gi/92090635	733	52	12	680	48	12	*	6	2
RYBP	gi/5381327	413	35	8	605	78	13	-	-	-
CBX7	gi/14867267	299	29	10	-	-	-	229	20	6
NSPC1	gi/37574111	-	-	-	165	29	6	-	-	-
MBLR	gi/28076973	-	-	-	366	31	13	97	6	2

C

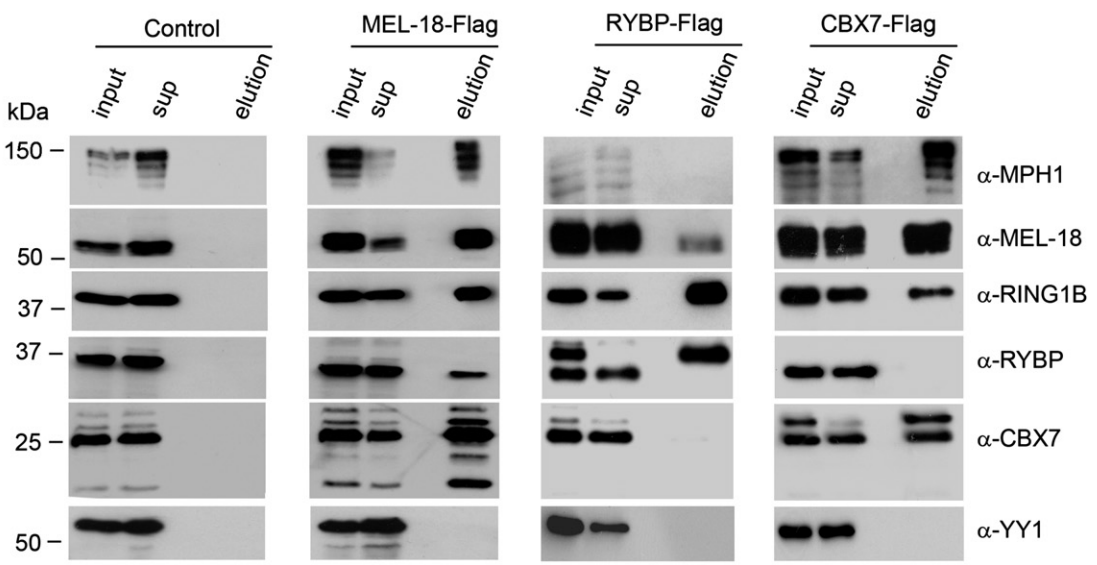

Figure 4. Proteomic Analysis of MEL-18, RYBP, and CBX7 Complexes in mESCs

(A) Silver-stained SDS polyacrylamide gel of control, MEL-18-Flag, RYBP-Flag, and CBX7-Flag purifications. PRC1 subunits identified by mass spectrometry of excised bands are indicated.

(B) Table showing the PRC1 core subunits copurifying with MEL-18-Flag, RYBP-Flag, and CBX7-Flag, as identified by mass spectrometry analysis. [1]Mascot score for specified proteins, [2]number of unique peptides identified. *The two peptides matched to RING1A are also present in RING1B.

(C) MEL-18-Flag, RYBP-Flag, and CBX7-Flag purifications analyzed by western blot with the indicated antibodies.

See also Figure S4.

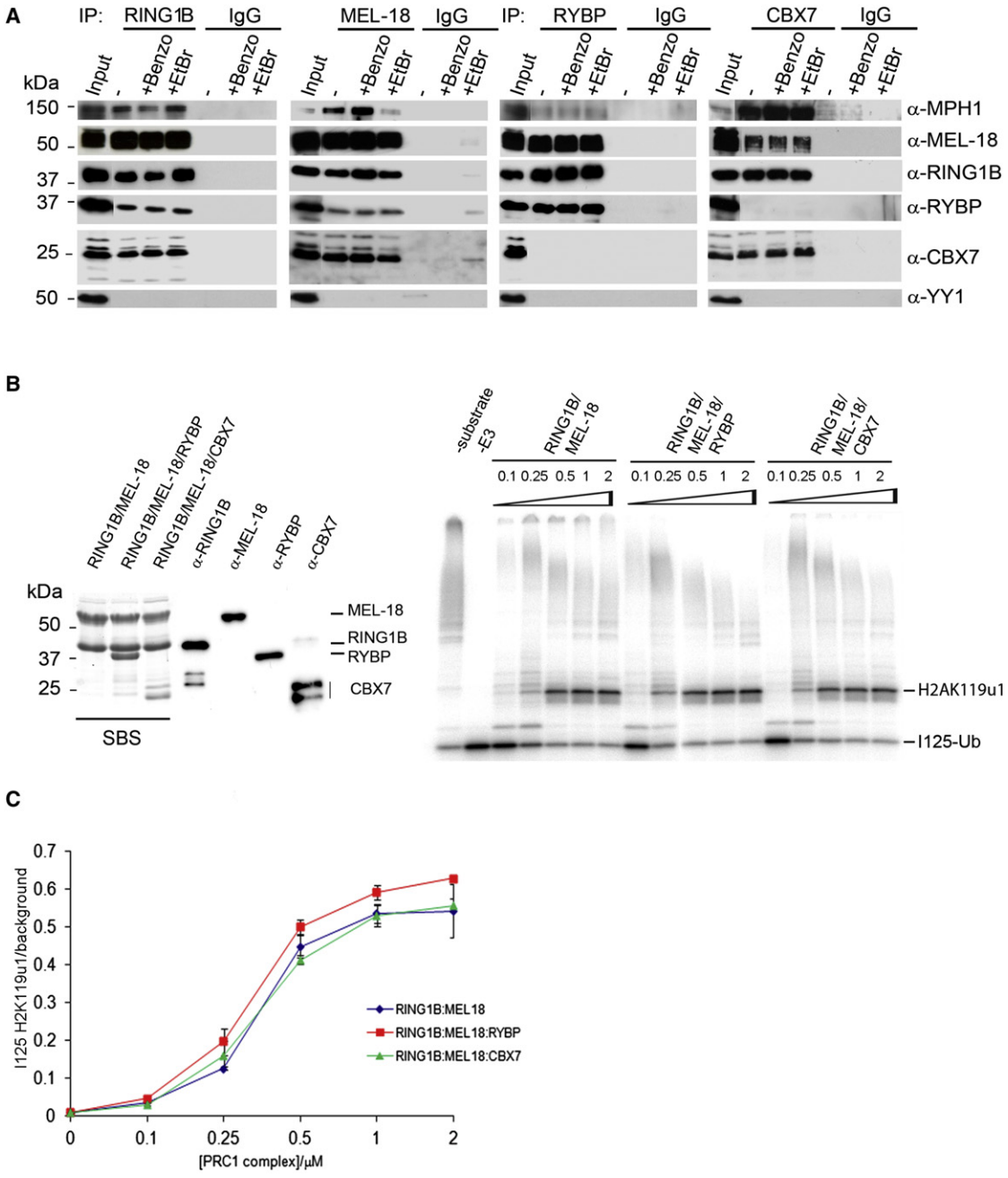

Figure 5. MEL-18 Interacts with RYBP and CBX7 in Mutually Exclusive Catalytically Active Complexes

(A) CoIP of endogenous RING1B, MEL-18, RYBP, and CBX7 from Eed4 WT mESC nuclear extracts, analyzed by western blot with the indicated antibodies and the appropriate IgG control. Benzonase (Benzo) and ethidium bromide (EtBr) were added where indicated. 10% input and 15% of RING1B, MEL-18, RYBP, CBX7, and the appropriate control CoIP are shown.

(B) Left panel: RING1B/MEL-18, RING1B/MEL-18/RYBP, and RING1B/MEL-18/CBX7 protein complexes analyzed by western blot using antibodies as indicated, or by Simply Blue Safe staining (SBS). Right panel: Ubiquitylation assays performed using indicated concentrations of RING1B/MEL-18 (lanes 3–7), RING1B/MEL-18/RYBP (lanes 8–12), and RING1B/MEL-18/CBX7 (lanes 13–17) complexes. Control assays are with substrate omitted or E3 ligase omitted. I^{125}-ubiquitin-labeled products are shown.

(C) Quantitation of H2AK119u1 from three independent assays as shown in (B).

See also Figure S5.

between Eed4 WT (Figure 5A), and Eed4 cKO mESCs (Figure S5A). These results demonstrate mutually exclusive binding of CBX7 and RYBP subunits and define the existence of two distinct PRC1-like complexes comprising, on the one hand, RING1B, MEL-18, CBX7, and MPH1 and, on the other, RING1B, MEL-18, and RYBP. We refer to these complexes henceforth as CBX-PRC1 and RYBP-PRC1. CoIP experiments in a mouse fibroblast cell line also revealed mutually exclusive interaction of CBX7 and RYBP with RING1B/MEL-18 (Figure S5B), indicating that RYBP-PRC1 and CBX-PRC1 coexist in different cell types.

To further investigate the composition of CBX-PRC1 and RYBP-PRC1, we established mESC lines expressing epitope-tagged RYBP or CBX7 and then purified the associated proteins. For RYBP (Figures 4A, panel 3 and 4B), we copurified RING1A/B and MEL-18. CBX proteins, including CBX7, were not detected at all. We did, however, copurify NSPC1 and MBLR, homologs of MEL-18 that are components of the BCOR and E2F6 complexes, respectively. This finding is consistent with the previously reported association of RYBP with these complexes (Gearhart et al., 2006; Ogawa et al., 2002; Sánchez et al., 2007; Trimarchi et al., 2001). Western analysis confirmed the presence of the major components RING1A/B and MEL-18 (Figure 4C, panel 3). YY1 was not identified in RYBP-Flag immunoprecipitates, either by proteomic or by western blot analysis. Purification of epitope-tagged CBX7 identified RING1A/B and MEL-18 as major components (Figures 4A, panel 4 and 4B). Western blot analysis confirmed these associations and demonstrated presence of MPH1 (Figure 4C, panel 4). RYBP was not detected. Taken together these results substantiate that RYBP-PRC1 and CBX-PRC1 are distinct multiprotein complexes.

The activity of PRC1 complexes in H2AK119 ubiquitylation requires a minimal catalytic core comprising RING1A/B together with MEL-18/BMI-1 (Cao et al., 2005; Elderkin et al., 2007). To determine whether RYBP-PRC1, which includes both RING1B and MEL-18 subunits, functions as an E3 ligase for H2AK119u1, we reconstituted RYBP-PRC1 (RING1B, MEL-18, and RYBP) and CBX-PRC1 (RING1B, MEL-18, and CBX7) using recombinant subunits (Figure 5B, left panel) and then carried out H2A ubiquitylation assays on oligonucleosome substrate (Figure 5B, right panel). As a control, we assayed the two-component complex comprising RING1B and MEL18 that in previous studies was shown to specifically monoubiquitylate H2AK119 (Elderkin et al., 2007). All three complexes efficiently monoubiquitylated H2A (Figure 5B, right panel), and quantitative analysis demonstrated equivalent activity in all cases (Figure 5C). Thus, RYBP and CBX proteins neither stimulate nor block H2A ubiquitylation activity of PRC1 complexes in vitro.

RYBP-PRC1 Mediates H2AK119u1 Independently of H3K27me3

To determine whether RYBP-PRC1 could account for H3K27me3-independent H2AK119u1, we carried out ChIP analysis for RYBP in Eed4 WT and Eed4 cKO mESCs. As shown in Figure 6A, RYBP enrichment relative to control loci was observed at several PcG target loci and, importantly, was unaffected following conditional depletion of H3K27me3 (Figure 6A). This mirrors results obtained for H2AK119u1 and contrasts with the effect on occupancy of RING1B and MEL-18 (Figure 1A). Similar results were obtained comparing constitutive *Eed*$^{-/-}$ mESCs relative to *Eed*$^{+/+}$ controls (Figure S6A) and in MG132-treated cells (Figure S6B), the latter demonstrating that H2AK119u1 is not required for RYBP occupancy.

To confirm these findings, we carried out ChIP-seq analysis of RYBP and CBX7 occupancy in *Eed*$^{+/+}$ and *Eed*$^{-/-}$ mESCs. Consistent with conventional ChIP analysis, we observed enrichment of RYBP over TSS of RING1B target loci, in both *Eed*$^{+/+}$ and *Eed*$^{-/-}$ mESCs (Figure 6B, panel 1). CBX7 occupancy on the other hand was only observed in *Eed*$^{+/+}$ cells (Figures 6B, panel 1 and S6C). There was no enrichment for RYBP or CBX7 at TSS associated with non-RING1B target loci (Figure 6B, panel 2). We conclude that RYBP-PRC1 occupancy at PcG target loci is independent of H3K27me3, providing an explanation for the maintenance of H2A119u1 levels and associated target gene silencing in PRC2-deficient mESCs.

PRC1-mediated H2AK119u1 is a marker of the inactive X chromosome (Xi) (de Napoles et al., 2004) and occurs in both the presence and the absence of H3K27me3 (Schoeftner et al., 2006). Moreover, a previous study observed RYBP localization to Xi in XX trophoblast stem cells (Arrigoni et al., 2006). To investigate whether RYBP-PRC1 could account for H3K27me3-independent H2AK119u1 on Xi, we performed RYBP immunofluorescence (IF) in mESCs that carry an autosomally located inducible *Xist* transgene on an *Eed*$^{-/-}$ background (36$^{Eed-/-}$) or rescued with an *Eed* transgene (36^{EedTg}) (Schoeftner et al., 2006). Xist RNA territories were counterstained with antisera specific for H2AK119u1. RYBP enrichment over the Xist RNA territory was observed in both rescued and *Eed*$^{-/-}$ mESCs (Figure 7A, left), and scoring data indicate that the levels are equivalent (Figure 7A, right). These observations suggest that RYBP-PRC1 is recruited in response to Xist RNA expression and that this accounts for H3K27me3-independent H2AK119u1 on Xi.

To directly test the role of RYBP in maintaining levels of H2AK119u1, we analyzed *Eed*$^{+/+}$ and *Eed*$^{-/-}$ mESCs in which we expressed one of two different shRNA hairpins to deplete RYBP levels (Figure 7B). In *Eed*$^{+/+}$ mESCs, RYBP knockdown led to substantially reduced levels of H2AK119u1 (Figure 7B, left). A smaller effect was observed with *Eed*$^{-/-}$ mESCs (Figure 7B, right), although it was difficult to derive stable undifferentiated mESCs in this case, indicating selection for mESCs in which RYBP depletion is ineffective. Interestingly, we observed a marked reduction in the levels of RING1B in RYBP knockdown cells (Figure 7B), suggesting that RYBP is important for the stabilization of RING1B. A similar effect is seen in cells depleted for PRC2 core components (Pasini et al., 2007; Silva et al., 2003). In line with reduced global levels of RING1B, we observed reduced occupancy of RING1B at PcG target loci (Figure S7B). In sum, these data demonstrate a central role for RYBP in mediating H2AK119u1.

DISCUSSION

RYBP-PRC1 Polycomb-Repressive Complex

RYBP was first identified in a yeast two-hybrid screen for RING1A and was further shown to interact with the transcription

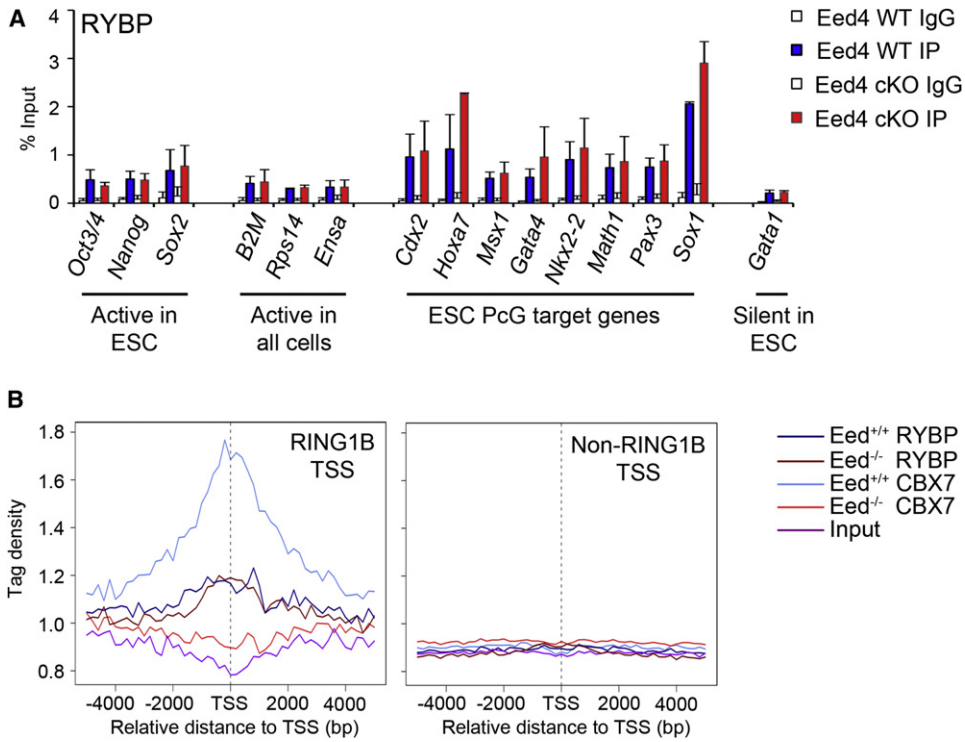

Figure 6. RYBP-PRC1 Is Recruited to PcG Target Genes Independently of PRC2

(A) ChIP analysis of RYBP in Eed4 WT and Eed4 cKO mESCs, showing average values + SD (n = 3).

(B) Tag density across the TSS of 20 million reads randomly subsampled. RYBP, CBX7, and input tags were clustered in two different subgroups, RING1B TSS and non-RING1B TSS (see Figure 2B). Data are shown for both *Eed*$^{+/+}$ and *Eed*$^{-/-}$ mESCs.

See also Figure S6.

factor YY1 (García et al., 1999). The latter finding is consistent with a previous study that identified YAF2, a close homolog of RYBP, as a YY1 interactor (Kalenik et al., 1997). Subsequent studies identified RYBP as having a role in apoptosis (Zheng et al., 2001). At present it is not clear whether these different ascribed functions and associations can be reconciled or whether RYBP is in fact multifunctional and participates in distinct pathways, interacting with different factors. Genetic studies in mouse demonstrate that RYBP is essential for early embryogenesis (Pirity et al., 2005), and close homologs are found in many species. Interestingly, RYBP mutations in *Drosophila* do not give a Polycomb phenotype (Bejarano et al., 2005). The presence in vertebrates of YAF2 adds further complexity to considerations of function.

Given the known interaction of RYBP with RING1A/B, copurification with PRC1 proteins was on one level unsurprising. Indeed RYBP/YAF2 has been identified as a component of BCOR (Gearhart et al., 2006; Sánchez et al., 2007) and E2F6 complexes (Sánchez et al., 2007; Trimarchi et al., 2001), together with RING1B and the mammalian PSC homologs NSPC1 and MBLR, respectively (Ogawa et al., 2002; Sánchez et al., 2007). However, homologs of other *Drosophila* PRC1 core subunits, PH and PC, were absent in these purifications, and moreover a number of independent analyses of PRC1 have not identified RYBP (Cao et al., 2005; Eskeland et al., 2010; Maertens et al., 2009; Saurin et al., 2001; Shao et al., 1999; Wang et al., 2004). In some cases this can be attributed retrospectively to the use of strategies based on epitope tagging of CBX proteins (Maertens et al., 2009; Ren and Kerppola, 2011; Saurin et al., 2001). In other instances, however, purifications were based on an H2A ubiquitylation activity assay (Wang et al., 2004) or epitope tagging of other PRC1 components (Cao et al., 2005; Eskeland et al., 2010; Maertens et al., 2009; Saurin et al., 2001; Shao et al., 1999; Wang et al., 2004). Notably, RYBP was not identified in previous purifications of PRC1 via epitope-tagged MEL-18 (Elderkin et al., 2007; Maertens et al., 2009). We assume this is attributable to technical factors as our analysis demonstrates that RYBP-PRC1 is present in mESCs and in different cell types. BMI-1, a second PSC homolog present in conventional PRC1 complexes, also copurifies stoichiometric levels of RYBP in mESCs and mouse NSCs (mNSCs) (data not shown), supporting a wider significance of RYBP-PRC1 complexes.

The fact that we see reciprocal immunoprecipitation of RYBP and MEL-18 in native extracts confirms that this interaction is physiologically relevant. Importantly, we show that the RYBP-PRC1 complex comprising RING1B, MEL-18, and RYBP can monoubiquitylate H2A on nucleosome substrates in vitro and that the activity of the complex is equivalent to that of CBX-PRC1.

In line with prior evidence (García et al., 1999; Wang et al., 2010), we find that interaction of RYBP and CBX7 with RING1B is mutually exclusive. We assume that the same is true for other

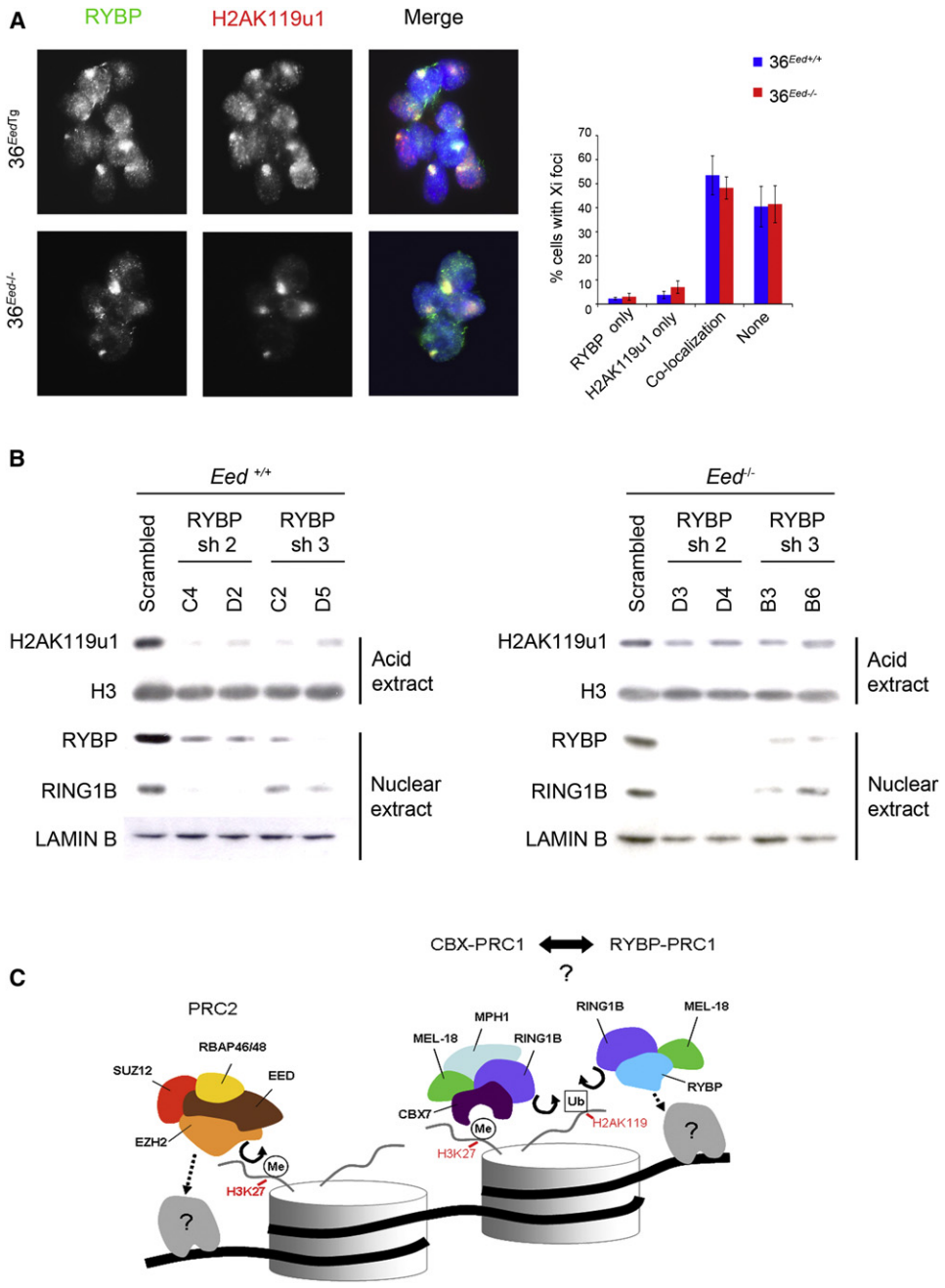

Figure 7. RYBP-PRC1 Is Recruited to Xist RNA Territories Independently of H3K27me3 and Is Required for H2AK119 Ubiquitylation in *Eed*$^{+/+}$ and *Eed*$^{-/-}$ mESCs

(A) Immunofluorescence analysis of RYBP (green) and H2AK119u1 (red) in 36^{EedTg} and $36^{Eed-/-}$ mESCs induced to express transgenic Xist RNA. DNA was counterstained with DAPI (blue). Graphs illustrate the proportion of cells in which H2AK119u1 foci and RYBP foci colocalize, based on scoring 100 cells on each of three separate slides.

(B) Stable cell lines were established following transduction of *Eed*$^{+/+}$ and *Eed*$^{-/-}$ mESCs with scrambled or either of two independent RYBP shRNAs (sh2 and sh3). Acid extracted histones (H2AK119u1 and H3) or nuclear extracts (RYBP, RING1B, and LAMIN B), were prepared and analyzed by western blot.

(C) Model as discussed in text. Key: DNA (black line); nucleosomes with single N terminus of H3 and C terminus of H2A (cylinders); H3K27 trimethylation (Me); H2AK119u1 (Ub); recruitment factors (gray shape with ?).

See also Figure S7.

mammalian homologs of *Drosophila* PC, specifically CBX2, 4, 6, and 8, but this has not been tested. We also observed that RYBP-PRC1 has a reduced association with MPH1. Consistent with this, RING1B but not MPH1/2 localizes to Xist RNA territories in *Eed*-deficient mESCs (Schoeftner et al., 2006). We assume that RYBP-PRC1 excludes other mammalian homologs of *Drosophila* PH, MPH2 and MPH3, but this also is untested. PH has been reported to interact with PSC (Kyba and Brock, 1998), and therefore to explain near exclusion of MPH1 from RYBP-PRC1, we speculate that RYBP occludes the required interaction surface on MEL-18.

Collectively our observations indicate that RYBP-PRC1 is comprised of three core components, RYBP, RING1B, and MEL-18/BMI-1. Our proteomic studies using epitope-tagged MEL-18 (this study) and BMI-1 (not shown) did not reveal other stoichiometric components, although we cannot rule out the presence of other key components at substoichiometric levels. Additionally, although in mESCs MEL-18 is an abundant PSC homolog, we cannot rule out a significant contribution of BMI-1 or other PSC homologs to RYBP-PRC1. Indeed, mESC RYBP complexes included the PSC homologs NSPC1 and MBLR, associated with BCOR and E2F6 complexes, respectively (Gearhart et al., 2006; Ogawa et al., 2002; Sánchez et al., 2007; Trimarchi et al., 2001). Studies in *Drosophila* have shown that the PRC1-related complex dRAF, comprised of RING1, PSC, and KDM2, plays a central role in global H2AK119u1 (Lagarou et al., 2008). This provides an interesting parallel with mESCs in which the BCOR complex includes a mammalian homolog of KDM2, KDM2B (Gearhart et al., 2006; Sánchez et al., 2007). However, there is no evidence that RYBP in *Drosophila* participates in PRC1-related complexes.

Recruitment of RYBP-PRC1

Genome-wide analysis of RING1B binding in the absence of H3K27me3 indicates that RYBP-PRC1 and PRC2 are recruited to many of the same target genes. It is intriguing that distribution of RING1B, localizing across CpG islands, resembles that of PRC2, even in the absence of H3K27me3. Indeed a recent study has suggested that unmethylated CpG domains may be sufficient to recruit PRC2 (Mendenhall et al., 2010). Although it is possible that the same signature recruits RYBP-PRC1, our analysis demonstrates sites bound by RING1B only in the presence of H3K27me3 and other sites where H3K27me3 is less important for RING1B targeting. Collectively, these observations suggest some differences in the targeting mechanisms of PRC2 and RYBP-PRC1, or at least in the relative contribution of the two pathways at specific loci.

Given that RYBP-PRC1 and PRC2 have significantly overlapping targets, can RYBP provide clues as to how targeting is mediated? As discussed above, RYBP was previously shown to interact with the transcription factor YY1 (García et al., 1999). Interestingly YY1 is the mammalian homolog of *Drosophila* PHO, which in the context of the PHO-RC complex plays a central role in PcG targeting (Klymenko et al., 2006). However, we did not find YY1 together with PRC1 in proteomic or native immunoprecipitation analyses. Moreover mapping of YY1-binding sites in mESCs reveals no significant overlap with PRC2 binding (Squazzo et al., 2006). We therefore conclude that interaction of RYBP with YY1 is unlikely to be relevant, at least in mESCs.

RYBP has a single conserved domain, a Ranbp2 zinc finger (Ranbp2-ZnF). A subset of proteins with this domain are associated with RNA metabolism, and moreover, nuclear magnetic resonance (NMR) studies have demonstrated that the Ranbp2-ZnF in these proteins binds RNA (Nguyen et al., 2011). This is potentially interesting in light of recruitment of RYBP in response to Xist RNA expression and also a series of recent studies suggesting a wider role for noncoding RNA in PcG recruitment (reviewed in Pauli et al., 2011). Arguing against this, comparative analysis indicates that the RYBP Ranbp2-ZnF belongs to a different class and that none of the contact residues for RNA binding are conserved or similar (not shown). A further subset of Ranbp2-ZnF proteins interact with ubiquitin, also characterized at the structural level (Wang et al., 2003), and here RYBP does show greater similarity. Indeed, it has been suggested that RYBP interacts with H2AK119u1 and additionally is subject to self-monoubiquitylation as a consequence of being in complex with RING1B (Arrigoni et al., 2006). This could be argued to point to a role for RYBP-PRC1 in maintaining H2AK119u1 by interacting with pre-existing marks on neighboring nucleosomes. However, our observation that RYBP is not displaced and that H2AK119u1 can be re-established following depletion by MG132 treatment, in both the presence and the absence of H3K27me3, appears to discount this idea. In sum, involvement of RYBP provides some intriguing clues that may help to understand PcG targeting, but further studies are needed to determine which, if any, are relevant.

Interplay of PRCs

Our data suggest that parallel pathways target H2A ubiquitylation to PcG targets in mESCs and on the inactive X chromosome. A model illustrating this is shown in Figure 7C. As discussed, the primary signal that recruits PRC2 and RYBP-PRC1 is unknown. CBX-PRC1 recruitment, on the other hand, is linked to PRC2-mediated H3K27me3. Although RYBP-PRC1 recruitment can occur in the absence of H3K27me3, we cannot rule out that CBX-PRC1 binding is at least partially dependent on RYBP-PRC1. In support of this view, we observed significant reduction of H2AK119u1 following RYBP knockdown in $Eed^{+/+}$ mESCs. Linked to this point, it is notable that reduced occupancy of RING1B and MEL-18 in PRC2-deficient mESCs is not mirrored by a greater reduction in global and local H2AK119u1 levels. One possible explanation is that RYBP-PRC1 has a short residence time on chromatin (relative to CBX-PRC1), sufficient for catalysis but not for efficient formaldehyde crosslinking, as has been observed for the interaction of the methylated DNA-binding protein MeCp2 with meCpG (Schmiedeberg et al., 2009).

Parallel targeting of RYBP-PRC1 and CBX-PRC1 provides an explanation for the fact that PRC2 null mESCs self-renew and retain pluripotency (Faust et al., 1998; O'Carroll et al., 2001; Pasini et al., 2004), whereas RING1A/B double-knockout cells (PRC1 null) cannot self-renew and therefore differentiate (Endoh et al., 2008). This may be a somewhat simplistic interpretation as mESCs lacking the PRC2 subunit SUZ12 (Pasini et al., 2004), and also cells in which both RING1B and EED are deleted (Leeb et al., 2010), show aberrant differentiation phenotypes.

Moreover, recent studies have shown that depletion of JARID2, a PRC2-associated cofactor, blocks differentiation of mESCs (reviewed in Herz and Shilatifard, 2010), as does *Jarid2* deletion (Landeira et al., 2010).

The fact that we see involvement of RYBP-PRC1 in Xist RNA-mediated silencing suggests a wider role for this complex. In future studies it will be interesting to determine whether RYBP has a role in other instances of H3K27me3-independent recruitment of PRC1 complexes, for example on paternal chromosomes in early preimplantation mouse embryos (Puschendorf et al., 2008).

EXPERIMENTAL PROCEDURES

Cell Culture

mESCs, FSPE fibroblasts, and NSCs were cultivated using established methods. Stable lines expressing Flag-tagged proteins were produced by lipofection followed by selection for antibiotic resistance. Full details are provided in the Extended Experimental Procedures. Pluripotency assays were performed using the alkaline phosphatase detection kit (Millipore).

ChIP and ChIP-Seq

ChIP was performed essentially as described (Stock et al., 2007) with some modifications used for specific antibodies, as detailed in the Extended Experimental Procedures. Results were analyzed either by qPCR or ChIP-seq as indicated. ChIP-seq was either by single- or paired-end methods as detailed in the Extended Experimental Procedures. Tags were mapped using bowtie (Langmead et al., 2009) excluding nonunique mappings (-m 1). Following alignment to the mouse genome (mm9), data were visualized on UCSC (Kent et al., 2002) and GBrowse (Stein et al., 2002). Single and paired-end tags were mapped on GBrowse, and peak identification was performed with MACS (Zhang et al., 2008) with a false discovery rate (FDR) < 2% and number of tags in the peak > 100. Nearest gene and overlaps to location used Cisgenome (Ji et al., 2008) and custom scripts. Peak intersection analysis used intersectBed (Quinlan and Hall, 2010) with CpG island data downloaded from UCSC mm9 table browser. Average profile across TSS used CEAS (Shin et al., 2009) after normalizing by random subsampling. For RYBP and CBX7 datasets, random subsampling was applied to RING1B and non-RING1B peaks selected from RING1B ChIP-seq peak list in the $Eed^{+/+}$ sample. Tag density analysis was performed with sitepro, part of the CEAS package, (Shin et al., 2009). Full details are provided in the Extended Experimental Procedures.

Western Blot Analysis

Levels of histone modifications and nonhistone protein were determined by western blot analysis of acid-extracted proteins or nuclear extracts, respectively, using appropriate primary and secondary antibodies as detailed in the Extended Experimental Procedures.

Gene Expression Analysis

Expression levels of PcG target genes were determined by qRT-PCR using standard methods.

Biochemical Analysis

Purifications from nuclear extract were carried out as described previously (van den Berg et al., 2010). Protein identification was by LC-MS/MS on an LTQ Orbitrap Velos Mass spectrometer. Data were searched against Uniprot 2011.03 using Mascot software.

Size-exclusion chromatography was carried out on a Superose 6 gel filtration column as detailed in the Extended Experimental Procedures. Recombinant complexes comprising combinations of full-length MEL-18, RING1B, RYBP, and CBX7 were purified from Sf9 cells essentially as described (Elderkin et al., 2007), using the Bac-to-Bac system (Invitrogen). Full details are provided in the Extended Experimental Procedures. Ubiquitylation assays were performed as described previously (Elderkin et al., 2007) and as detailed in the Extended Experimental Procedures. Immunoprecipitations were from nuclear extracts (Dignam et al., 1983) using appropriate primary and secondary antibodies either without treatment or in the presence of benzonase or *EtBr* as described previously (van den Berg et al., 2010).

Immunofluorescence

Immunofluorescence (IF) was performed as described (de Napoles et al., 2004; Fang et al., 2004) with antibody dilutions, as detailed in the Extended Experimental Procedures. Images were acquired on a Zeiss AX10 microscope equipped with AxioCam MRm CCD camera using AxioVision software.

ACCESSION NUMBERS

ChIP sequencing data are available at GEO under accession number GSE23716. Primers used in this study are in Table S1.

SUPPLEMENTAL INFORMATION

Supplemental Information includes Extended Experimental Procedures and seven figures and can be found with this article online at doi:10.1016/j.cell.2011.12.029.

ACKNOWLEDGMENTS

We would like to thank members of the lab and Rob Klose and Len R. Stephens for discussion and advice. We thank Haruhiko Koseki for providing RING1B and MPH1 antibodies and for helpful discussions. We thank the High-Throughput Genomics Group at the Wellcome Trust Centre for Human Genetics (funded by Wellcome Trust grant reference 090532/Z/09/Z and MRC Hub grant G0900747 91070) for the generation of data. This work was funded by the Wellcome Trust, UK (N.B.; WT081385, S.E.; WT085102MA) and the BBSRC (E.D., D.O., and J.W.). L.T. received a PhD studentship from FCT, Portugal. M.V. is supported by grant BFU2010-18146 (Spanish Ministry of Science and Innovation) and Fundación Ramón Areces.

Received: May 19, 2011
Revised: October 19, 2011
Accepted: December 15, 2011
Published online: February 9, 2012

REFERENCES

Agger, K., Cloos, P.A.C., Christensen, J., Pasini, D., Rose, S., Rappsilber, J., Issaeva, I., Canaani, E., Salcini, A.E., and Helin, K. (2007). UTX and JMJD3 are histone H3K27 demethylases involved in HOX gene regulation and development. Nature *449*, 731–734.

Arrigoni, R., Alam, S.L., Wamstad, J.A., Bardwell, V.J., Sundquist, W.I., and Schreiber-Agus, N. (2006). The Polycomb-associated protein Rybp is a ubiquitin binding protein. FEBS Lett. *580*, 6233–6241.

Azuara, V., Perry, P., Sauer, S., Spivakov, M., Jørgensen, H.F., John, R.M., Gouti, M., Casanova, M., Warnes, G., Merkenschlager, M., and Fisher, A.G. (2006). Chromatin signatures of pluripotent cell lines. Nat. Cell Biol. *8*, 532–538.

Bejarano, F., González, I., Vidal, M., and Busturia, A. (2005). The Drosophila RYBP gene functions as a Polycomb-dependent transcriptional repressor. Mech. Dev. *122*, 1118–1129.

Boyer, L.A., Plath, K., Zeitlinger, J., Brambrink, T., Medeiros, L.A., Lee, T.I., Levine, S.S., Wernig, M., Tajonar, A., Ray, M.K., et al. (2006). Polycomb complexes repress developmental regulators in murine embryonic stem cells. Nature *441*, 349–353.

Cao, R., Wang, L., Wang, H., Xia, L., Erdjument-Bromage, H., Tempst, P., Jones, R.S., and Zhang, Y. (2002). Role of histone H3 lysine 27 methylation in Polycomb-group silencing. Science *298*, 1039–1043.

Cao, R., Tsukada, Y.-I., and Zhang, Y. (2005). Role of Bmi-1 and Ring1A in H2A ubiquitylation and Hox gene silencing. Mol. Cell *20*, 845–854.

Chamberlain, S.J., Yee, D., and Magnuson, T. (2008). Polycomb repressive complex 2 is dispensable for maintenance of embryonic stem cell pluripotency. Stem Cells *26*, 1496–1505.

Czypionka, A., de los Paños, O.R., Mateu, M.G., Barrera, F.N., Hurtado-Gómez, E., Gómez, J., Vidal, M., and Neira, J.L. (2007). The isolated C-terminal domain of Ring1B is a dimer made of stable, well-structured monomers. Biochemistry *46*, 12764–12776.

Dantuma, N.P., Groothuis, T.A.M., Salomons, F.A., and Neefjes, J. (2006). A dynamic ubiquitin equilibrium couples proteasomal activity to chromatin remodeling. J. Cell Biol. *173*, 19–26.

de Napoles, M., Mermoud, J.E., Wakao, R., Tang, Y.A., Endoh, M., Appanah, R., Nesterova, T.B., Silva, J., Otte, A.P., Vidal, M., et al. (2004). Polycomb group proteins Ring1A/B link ubiquitylation of histone H2A to heritable gene silencing and X inactivation. Dev. Cell *7*, 663–676.

Dignam, J.D., Lebovitz, R.M., and Roeder, R.G. (1983). Accurate transcription initiation by RNA polymerase II in a soluble extract from isolated mammalian nuclei. Nucleic Acids Res. *11*, 1475–1489.

Elderkin, S., Maertens, G.N., Endoh, M., Mallery, D.L., Morrice, N., Koseki, H., Peters, G., Brockdorff, N., and Hiom, K. (2007). A phosphorylated form of Mel-18 targets the Ring1B histone H2A ubiquitin ligase to chromatin. Mol. Cell *28*, 107–120.

Endoh, M., Endo, T.A., Endoh, T., Fujimura, Y.-i., Ohara, O., Toyoda, T., Otte, A.P., Okano, M., Brockdorff, N., Vidal, M., and Koseki, H. (2008). Polycomb group proteins Ring1A/B are functionally linked to the core transcriptional regulatory circuitry to maintain ES cell identity. Development *135*, 1513–1524.

Eskeland, R., Leeb, M., Grimes, G.R., Kress, C., Boyle, S., Sproul, D., Gilbert, N., Fan, Y., Skoultchi, A.I., Wutz, A., and Bickmore, W.A. (2010). Ring1B compacts chromatin structure and represses gene expression independent of histone ubiquitination. Mol. Cell *38*, 452–464.

Fang, J., Chen, T., Chadwick, B., Li, E., and Zhang, Y. (2004). Ring1b-mediated H2A ubiquitination associates with inactive X chromosomes and is involved in initiation of X inactivation. J. Biol. Chem. *279*, 52812–52815.

Faust, C., Lawson, K.A., Schork, N.J., Thiel, B., and Magnuson, T. (1998). The Polycomb-group gene eed is required for normal morphogenetic movements during gastrulation in the mouse embryo. Development *125*, 4495–4506.

Fischle, W., Wang, Y., Jacobs, S.A., Kim, Y., Allis, C.D., and Khorasanizadeh, S. (2003). Molecular basis for the discrimination of repressive methyl-lysine marks in histone H3 by Polycomb and HP1 chromodomains. Genes Dev. *17*, 1870–1881.

Francis, N.J., Saurin, A.J., Shao, Z., and Kingston, R.E. (2001). Reconstitution of a functional core polycomb repressive complex. Mol. Cell *8*, 545–556.

Francis, N.J., Kingston, R.E., and Woodcock, C.L. (2004). Chromatin compaction by a polycomb group protein complex. Science *306*, 1574–1577.

García, E., Marcos-Gutiérrez, C., del Mar Lorente, M., Moreno, J.C., and Vidal, M. (1999). RYBP, a new repressor protein that interacts with components of the mammalian Polycomb complex, and with the transcription factor YY1. EMBO J. *18*, 3404–3418.

Gearhart, M.D., Corcoran, C.M., Wamstad, J.A., and Bardwell, V.J. (2006). Polycomb group and SCF ubiquitin ligases are found in a novel BCOR complex that is recruited to BCL6 targets. Mol. Cell. Biol. *26*, 6880–6889.

Hansen, K.H., Bracken, A.P., Pasini, D., Dietrich, N., Gehani, S.S., Monrad, A., Rappsilber, J., Lerdrup, M., and Helin, K. (2008). A model for transmission of the H3K27me3 epigenetic mark. Nat. Cell Biol. *10*, 1291–1300.

Herz, H.M., and Shilatifard, A. (2010). The JARID2-PRC2 duality. Genes Dev. *24*, 857–861.

Huen, D.S., and Russell, S. (2010). On the use of resampling tests for evaluating statistical significance of binding-site co-occurrence. BMC Bioinformatics *11*, 359.

Ji, H., Jiang, H., Ma, W., Johnson, D.S., Myers, R.M., and Wong, W.H. (2008). An integrated software system for analyzing ChIP-chip and ChIP-seq data. Nat. Biotechnol. *26*, 1293–1300.

Kalenik, J.L., Chen, D., Bradley, M.E., Chen, S.J., and Lee, T.C. (1997). Yeast two-hybrid cloning of a novel zinc finger protein that interacts with the multifunctional transcription factor YY1. Nucleic Acids Res. *25*, 843–849.

Kent, W.J., Sugnet, C.W., Furey, T.S., Roskin, K.M., Pringle, T.H., Zahler, A.M., and Haussler, D. (2002). The human genome browser at UCSC. Genome Res. *12*, 996–1006.

King, I.F.G., Francis, N.J., and Kingston, R.E. (2002). Native and recombinant polycomb group complexes establish a selective block to template accessibility to repress transcription in vitro. Mol. Cell. Biol. *22*, 7919–7928.

Klymenko, T., Papp, B., Fischle, W., Köcher, T., Schelder, M., Fritsch, C., Wild, B., Wilm, M., and Müller, J. (2006). A Polycomb group protein complex with sequence-specific DNA-binding and selective methyl-lysine-binding activities. Genes Dev. *20*, 1110–1122.

Ku, M., Koche, R.P., Rheinbay, E., Mendenhall, E.M., Endoh, M., Mikkelsen, T.S., Presser, A., Nusbaum, C., Xie, X., Chi, A.S., et al. (2008). Genomewide analysis of PRC1 and PRC2 occupancy identifies two classes of bivalent domains. PLoS Genet. *4*, e1000242.

Kyba, M., and Brock, H.W. (1998). The Drosophila polycomb group protein Psc contacts ph and Pc through specific conserved domains. Mol. Cell. Biol. *18*, 2712–2720.

Lagarou, A., Mohd-Sarip, A., Moshkin, Y.M., Chalkley, G.E., Bezstarosti, K., Demmers, J.A.A., and Verrijzer, C.P. (2008). dKDM2 couples histone H2A ubiquitylation to histone H3 demethylation during Polycomb group silencing. Genes Dev. *22*, 2799–2810.

Landeira, D., Sauer, S., Poot, R., Dvorkina, M., Mazzarella, L., Jørgensen, H.F., Pereira, C.F., Leleu, M., Piccolo, F.M., Spivakov, M., et al. (2010). Jarid2 is a PRC2 component in embryonic stem cells required for multi-lineage differentiation and recruitment of PRC1 and RNA Polymerase II to developmental regulators. Nat. Cell Biol. *12*, 618–624.

Langmead, B., Trapnell, C., Pop, M., and Salzberg, S.L. (2009). Ultrafast and memory-efficient alignment of short DNA sequences to the human genome. Genome Biol. *10*, R25.

Lee, M.G., Villa, R., Trojer, P., Norman, J., Yan, K.-P., Reinberg, D., Di Croce, L., and Shiekhattar, R. (2007). Demethylation of H3K27 regulates polycomb recruitment and H2A ubiquitination. Science *318*, 447–450.

Leeb, M., Pasini, D., Novatchkova, M., Jaritz, M., Helin, K., and Wutz, A. (2010). Polycomb complexes act redundantly to repress genomic repeats and genes. Genes Dev. *24*, 265–276.

Maertens, G.N., El Messaoudi-Aubert, S., Racek, T., Stock, J.K., Nicholls, J., Rodriguez-Niedenführ, M., Gil, J., and Peters, G. (2009). Several distinct polycomb complexes regulate and co-localize on the INK4a tumor suppressor locus. PLoS ONE *4*, e6380.

Margueron, R., Justin, N., Ohno, K., Sharpe, M.L., Son, J., Drury, W.J., 3rd, Voigt, P., Martin, S.R., Taylor, W.R., De Marco, V., et al. (2009). Role of the polycomb protein EED in the propagation of repressive histone marks. Nature *461*, 762–767.

Mendenhall, E.M., Koche, R.P., Truong, T., Zhou, V.W., Issac, B., Chi, A.S., Ku, M., and Bernstein, B.E. (2010). GC-rich sequence elements recruit PRC2 in mammalian ES cells. PLoS Genet. *6*, e1001244.

Mikkelsen, T.S., Ku, M., Jaffe, D.B., Issac, B., Lieberman, E., Giannoukos, G., Alvarez, P., Brockman, W., Kim, T.-K., Koche, R.P., et al. (2007). Genome-wide maps of chromatin state in pluripotent and lineage-committed cells. Nature *448*, 553–560.

Min, J., Zhang, Y., and Xu, R.-M. (2003). Structural basis for specific binding of Polycomb chromodomain to histone H3 methylated at Lys 27. Genes Dev. *17*, 1823–1828.

Mujtaba, S., Manzur, K.L., Gurnon, J.R., Kang, M., Van Etten, J.L., and Zhou, M.-M. (2008). Epigenetic transcriptional repression of cellular genes by a viral SET protein. Nat. Cell Biol. *10*, 1114–1122.

Müller, J., and Verrijzer, P. (2009). Biochemical mechanisms of gene regulation by polycomb group protein complexes. Curr. Opin. Genet. Dev. *19*, 150–158.

Nguyen, C.D., Mansfield, R.E., Leung, W., Vaz, P.M., Loughlin, F.E., Grant, R.P., and Mackay, J.P. (2011). Characterization of a family of RanBP2-type

zinc fingers that can recognize single-stranded RNA. J. Mol. Biol. *407*, 273–283.

O'Carroll, D., Erhardt, S., Pagani, M., Barton, S.C., Surani, M.A., and Jenuwein, T. (2001). The polycomb-group gene Ezh2 is required for early mouse development. Mol. Cell. Biol. *21*, 4330–4336.

Ogawa, H., Ishiguro, K.-I., Gaubatz, S., Livingston, D.M., and Nakatani, Y. (2002). A complex with chromatin modifiers that occupies E2F- and Myc-responsive genes in G0 cells. Science *296*, 1132–1136.

Pasini, D., Bracken, A.P., Jensen, M.R., Lazzerini Denchi, E., and Helin, K. (2004). Suz12 is essential for mouse development and for EZH2 histone methyltransferase activity. EMBO J. *23*, 4061–4071.

Pasini, D., Bracken, A.P., Hansen, J.B., Capillo, M., and Helin, K. (2007). The polycomb group protein Suz12 is required for embryonic stem cell differentiation. Mol. Cell. Biol. *27*, 3769–3779.

Pauli, A., Rinn, J.L., and Schier, A.F. (2011). Non-coding RNAs as regulators of embryogenesis. Nat. Rev. Genet. *12*, 136–149.

Pirity, M.K., Locker, J., and Schreiber-Agus, N. (2005). Rybp/DEDAF is required for early postimplantation and for central nervous system development. Mol. Cell. Biol. *25*, 7193–7202.

Puschendorf, M., Terranova, R., Boutsma, E., Mao, X., Isono, K.-i., Brykczynska, U., Kolb, C., Otte, A.P., Koseki, H., Orkin, S.H., et al. (2008). PRC1 and Suv39h specify parental asymmetry at constitutive heterochromatin in early mouse embryos. Nat. Genet. *40*, 411–420.

Quinlan, A.R., and Hall, I.M. (2010). BEDTools: a flexible suite of utilities for comparing genomic features. Bioinformatics *26*, 841–842.

Ren, X., and Kerppola, T.K. (2011). REST interacts with Cbx proteins and regulates polycomb repressive complex 1 occupancy at RE1 elements. Mol. Cell. Biol. *31*, 2100–2110.

Sánchez, C., Sánchez, I., Demmers, J.A.A., Rodriguez, P., Strouboulis, J., and Vidal, M. (2007). Proteomics analysis of Ring1B/Rnf2 interactors identifies a novel complex with the Fbxl10/Jhdm1B histone demethylase and the Bcl6 interacting corepressor. Mol. Cell. Proteomics *6*, 820–834.

Saurin, A.J., Shao, Z., Erdjument-Bromage, H., Tempst, P., and Kingston, R.E. (2001). A Drosophila Polycomb group complex includes Zeste and dTAFII proteins. Nature *412*, 655–660.

Schmiedeberg, L., Skene, P., Deaton, A., and Bird, A. (2009). A temporal threshold for formaldehyde crosslinking and fixation. PLoS ONE *4*, e4636.

Schoeftner, S., Sengupta, A.K., Kubicek, S., Mechtler, K., Spahn, L., Koseki, H.H., Jenuwein, T., and Wutz, A. (2006). Recruitment of PRC1 function at the initiation of X inactivation independent of PRC2 and silencing. EMBO J. *25*, 3110–3122.

Schwartz, Y.B., Kahn, T.G., Nix, D.A., Li, X.-Y., Bourgon, R., Biggin, M., and Pirrotta, V. (2006). Genome-wide analysis of Polycomb targets in Drosophila melanogaster. Nat. Genet. *38*, 700–705.

Shao, Z., Raible, F., Mollaaghababa, R., Guyon, J.R., Wu, C.T., Bender, W., and Kingston, R.E. (1999). Stabilization of chromatin structure by PRC1, a Polycomb complex. Cell *98*, 37–46.

Shen, X., Liu, Y., Hsu, Y.-J., Fujiwara, Y., Kim, J., Mao, X., Yuan, G.-C., and Orkin, S.H. (2008). EZH1 mediates methylation on histone H3 lysine 27 and complements EZH2 in maintaining stem cell identity and executing pluripotency. Mol. Cell *32*, 491–502.

Shin, H., Liu, T., Manrai, A.K., and Liu, X.S. (2009). CEAS: cis-regulatory element annotation system. Bioinformatics *25*, 2605–2606.

Silva, J., Mak, W., Zvetkova, I., Appanah, R., Nesterova, T.B., Webster, Z., Peters, A.H.F.M., Jenuwein, T., Otte, A.P., and Brockdorff, N. (2003). Establishment of histone h3 methylation on the inactive X chromosome requires transient recruitment of Eed-Enx1 polycomb group complexes. Dev. Cell *4*, 481–495.

Simon, J.A., and Kingston, R.E. (2009). Mechanisms of polycomb gene silencing: knowns and unknowns. Nat. Rev. Mol. Cell Biol. *10*, 697–708.

Squazzo, S.L., O'Geen, H., Komashko, V.M., Krig, S.R., Jin, V.X., Jang, S.W., Margueron, R., Reinberg, D., Green, R., and Farnham, P.J. (2006). Suz12 binds to silenced regions of the genome in a cell-type-specific manner. Genome Res. *16*, 890–900.

Stein, L.D., Mungall, C., Shu, S., Caudy, M., Mangone, M., Day, A., Nickerson, E., Stajich, J.E., Harris, T.W., Arva, A., and Lewis, S. (2002). The generic genome browser: a building block for a model organism system database. Genome Res. *12*, 1599–1610.

Stock, J.K., Giadrossi, S., Casanova, M., Brookes, E., Vidal, M., Koseki, H., Brockdorff, N., Fisher, A.G., and Pombo, A. (2007). Ring1-mediated ubiquitination of H2A restrains poised RNA polymerase II at bivalent genes in mouse ES cells. Nat. Cell Biol. *9*, 1428–1435.

Szutorisz, H., Georgiou, A., Tora, L., and Dillon, N. (2006). The proteasome restricts permissive transcription at tissue-specific gene loci in embryonic stem cells. Cell *127*, 1375–1388.

Trimarchi, J.M., Fairchild, B., Wen, J., and Lees, J.A. (2001). The E2F6 transcription factor is a component of the mammalian Bmi1-containing polycomb complex. Proc. Natl. Acad. Sci. USA *98*, 1519–1524.

Ura, H., Usuda, M., Kinoshita, K., Sun, C., Mori, K., Akagi, T., Matsuda, T., Koide, H., and Yokota, T. (2008). STAT3 and Oct-3/4 control histone modification through induction of Eed in embryonic stem cells. J. Biol. Chem. *283*, 9713–9723.

van den Berg, D.L., Snoek, T., Mullin, N.P., Yates, A., Bezstarosti, K., Demmers, J., Chambers, I., and Poot, R.A. (2010). An Oct4-centered protein interaction network in embryonic stem cells. Cell Stem Cell *6*, 369–381.

Wang, B., Alam, S.L., Meyer, H.H., Payne, M., Stemmler, T.L., Davis, D.R., and Sundquist, W.I. (2003). Structure and ubiquitin interactions of the conserved zinc finger domain of Npl4. J. Biol. Chem. *278*, 20225–20234.

Wang, H., Wang, L., Erdjument-Bromage, H., Vidal, M., Tempst, P., Jones, R.S., and Zhang, Y. (2004). Role of histone H2A ubiquitination in Polycomb silencing. Nature *431*, 873–878.

Wang, R., Taylor, A.B., Leal, B.Z., Chadwell, L.V., Ilangovan, U., Robinson, A.K., Schirf, V., Hart, P.J., Lafer, E.M., Demeler, B., et al. (2010). Polycomb group targeting through different binding partners of RING1B C-terminal domain. Structure *18*, 966–975.

Zhang, Y., Liu, T., Meyer, C.A., Eeckhoute, J., Johnson, D.S., Bernstein, B.E., Nusbaum, C., Myers, R.M., Brown, M., Li, W., and Liu, X.S. (2008). Model-based analysis of ChIP-Seq (MACS). Genome Biol. *9*, R137.

Zheng, L., Schickling, O., Peter, M.E., and Lenardo, M.J. (2001). The death effector domain-associated factor plays distinct regulatory roles in the nucleus and cytoplasm. J. Biol. Chem. *276*, 31945–31952.